

SPECTRALLY COMPATIBLE WAVEFORM DESIGN FOR MIMO RADAR TRANSMIT BEAMPATTERN WITH PAR AND SIMILARITY CONSTRAINTS

Ziyang Cheng, Zishu He, Min Fang, Jun Li, and Julian Xie

School of Electronic Engineering, UESTC, Chengdu 611731, China

Email: zeeyoungcheng@163.com

ABSTRACT

This paper investigates the problem of the spectrally compatible waveform design for multiple-in multiple-out (MIMO) radar transmit beampattern formation, subject to peak-to-average-power ratio (PAR) and waveform similarity constraints. Since the formulated optimization problem of minimizing the Integrate Sidelobe Level (ISL) and the waveform energy of the stop-band frequencies is NP-hard, an auxiliary variable is first introduced to modify the non-convex problem into a bi-quasiconvex problem, and then the approximated alternating directions method of multipliers (A-ADMM) algorithm is proposed to tackle the resulting bi-quasiconvex problem. Finally, numerical results are presented to evaluate the effectiveness of the proposed algorithm.

Index Terms— MIMO radar, spectrally compatible waveforms, transmit beampattern, PAR constraint, similarity constraint, A-ADMM.

1. INTRODUCTION

Unlike a conventional phased array radar transmitting single waveform, a MIMO radar can transmit multiple waveforms [1, 2]. Thanks to the waveform diversity, a MIMO radar has various advantages such as improved flexibility of transmit beampattern design [3]–[9], higher spatial resolution [10], [11], and better target detection capability [12], etc. Here, this paper focuses on the transmit beampattern design for a colocated MIMO radar.

Currently, the waveform design for MIMO radar beampattern formation has been received the great interest. The main approaches to deal with this problem can be generally classified into the two categories. The first one is synthesizing the transmit waveform via the two-step method. For example, in [3] the waveform covariance matrix is optimized to approximate the desired transmit beampattern and minimize sidelobe level using Semi-Definite Quadratic programming (SQP) technique, and then the Cyclic Algorithm (CA) is presented to deliver the waveform with a constant modulus or peak-to-average-power ratio (PAR) constraint in [4]. The second one

is designing the waveform through the one-step approach to obtain the desired beampattern. For instance, in [8], the transmit signal is obtained directly by solving the waveform matrix. In addition, in [9], two objective functions are considered to design the constant modulus waveforms directly based on the ADMM algorithm for beampattern formation.

However, the all above mentioned methods investigate the problem of the waveform design for transmit beampattern formation considering only the requirement of transmitter (i.e., the constant modulus or PAR constraint). In fact, the designed waveform is also required to share some good ambiguity properties of the reference waveform, therefore a similarity constraint is desirable [13, 14]. Moreover, the spectral coexistence condition is needed to satisfy the requirement for both radar and telecommunication systems [15]–[17].

In this paper, the problem of transmit beampattern design for a colocated MIMO radar is considered. Unlike the existing approaches for transmit beampattern design with only constant modulus constraint (or PAR constraint), the spectral compatibility, PAR and similarity constraints are imposed on the transmit waveform. In order to deal with the resulting problem with a non-convex quadratic equality constraint and quadratic inequality constraints, an auxiliary variable is introduced to modify the non-convex problem into a bi-quasiconvex problem. Subsequently, the A-ADMM algorithm is proposed to solve the modified problem by taking advantage of the block successive upper-bound minimization method (BSUM) [18] and the ADMM algorithm [19]. Under the proposed framework, we update the primal variables by minimizing an approximated function of the augmented Lagrangian function. Finally, numerical simulations are carried out to assess the waveform performance in terms of the beampattern, spectral shape and pulse compression properties.

2. PROBLEM FORMULATION

Consider a colocated MIMO radar with M transmit antennas. Each antenna emits a different waveform $s_m(l)$, $m = 1, \dots, M; l = 1, \dots, L$ with L being the number of discrete time samples of each pulse. Let $\mathbf{s}(l) = [s_1(l), s_2(l), \dots, s_M(l)]^T$ be the space transmit waveform in

This work was supported by the Fundamental Research Funds for the Central Universities ZYGX2016J027.

the l -th sample, where $(\cdot)^T$ denotes transpose operator, and $\mathbf{S} = [\mathbf{s}(1), \mathbf{s}(2), \dots, \mathbf{s}(L)]$ be the space-time transmit waveform matrix. The transmit beampattern in the spacial domain θ can be expressed as [9]

$$P(\theta) = \mathbf{s}^H \mathbf{R}(\theta) \mathbf{s} \quad (1)$$

where $(\cdot)^H$ denotes conjugate transpose operator, $\mathbf{s} = \text{vec}(\mathbf{S})$, and $\mathbf{R}(\theta)$ is given by

$$\mathbf{R}(\theta) = \mathbf{I}_L \otimes \mathbf{a}_T^*(\theta) \mathbf{a}_T^T(\theta) \quad (2)$$

with $\mathbf{a}_T(\theta)$ being the transmit steering vector.

Thus, the beampattern integrate sidelobe level (ISL) can be written as

$$\text{ISL} = \frac{\sum_{\theta \in \Theta_s} \mathbf{s}^H \mathbf{R}(\theta) \mathbf{s}}{\sum_{\theta \in \Theta_m} \mathbf{s}^H \mathbf{R}(\theta) \mathbf{s}} = \frac{\mathbf{s}^H \mathbf{\Upsilon}_s \mathbf{s}}{\mathbf{s}^H \mathbf{\Upsilon}_m \mathbf{s}} \quad (3)$$

where Θ_s and Θ_m represent the sidelobe region and main region, respectively. $\mathbf{\Upsilon}_s$ and $\mathbf{\Upsilon}_m$ are respectively defined as

$$\mathbf{\Upsilon}_s = \sum_{\theta \in \Theta_s} \mathbf{R}(\theta) \quad \text{and} \quad \mathbf{\Upsilon}_m = \sum_{\theta \in \Theta_m} \mathbf{R}(\theta)$$

In coexistent system of radar and communications, it is supposed that each communication system is operating over a frequency band $\Omega_k = [f_l^k, f_u^k]$, $k = 1, \dots, K$, where f_l^k and f_u^k denote the lower and upper normalized frequencies for the k -th system. The transmitted waveform energy in the k -th band can be computed as

$$\int_{f_l^k}^{f_u^k} Y(f) df = \tilde{\mathbf{s}}^H \mathbf{F}^k \tilde{\mathbf{s}} \quad (4)$$

where $Y(f)$ denotes the Energy Spectral Density (ESD) of the sum code of multiple waveforms $\tilde{\mathbf{s}}$, and the (m, n) th entry of \mathbf{F}^k is given by [15]

$$\mathbf{F}^k(m, l) = \begin{cases} f_u^k - f_l^k, & m = n \\ \frac{e^{j2\pi f_u^k(m-n)} - e^{j2\pi f_l^k(m-n)}}{j2\pi(m-n)}, & m \neq n \end{cases} \quad (5)$$

and $\tilde{\mathbf{s}}$ is

$$\tilde{\mathbf{s}} = \text{vec}(\mathbf{1}_M^T \mathbf{S}) = (\mathbf{I}_L \otimes \mathbf{1}_M^T) \mathbf{s} \quad (6)$$

Therefore, combining (6), (4) can be reexpressed as

$$\int_{f_l^k}^{f_u^k} Y(f) df = \mathbf{s}^H \mathbf{\Xi}^k \mathbf{s} \quad (7)$$

where $\mathbf{\Xi}^k = ((\mathbf{I}_L \otimes \mathbf{1}_M^T)^H \mathbf{F}^k (\mathbf{I}_L \otimes \mathbf{1}_M^T))$.

To proceed, in practice, the PAR constraint is considered for the transmit waveform [20], as

$$\frac{\max_l |s_m(l)|^2}{\frac{1}{L} \sum_{l=1}^L |s_m(l)|^2} \leq \eta, \quad \eta \in [1, L] \quad (8)$$

Specially, assuming the total transmit energy is 1 and the energy of each transmit antenna are the same, the PAR constraint in (8) can thus be rewritten as

$$\mathbf{s}^H \mathbf{s} = 1; \quad \mathbf{s}^H \mathbf{E}_n \mathbf{s} \leq \frac{\eta}{ML}, \quad n = 1, 2, \dots, ML \quad (9)$$

where $\mathbf{E}_n(i, j)$ is given by

$$\mathbf{E}_n(i, j) = \begin{cases} 1 & i = n \text{ and } j = n \\ 0 & \text{otherwise.} \end{cases} \quad (10)$$

More specially, when $\eta = 1$ the PAR constraint is reduced to the constant modulus constraint.

In addition, a similarity constraint is enforced on the designed waveform to share the good pulse compression property of the reference waveform. The L_2 norm similarity constraint can be written as [21]

$$\|\mathbf{s} - \mathbf{s}_0\|_2 \leq \varepsilon \quad (11)$$

where \mathbf{s}_0 denotes a reference waveform and ε is a user-defined parameter to control the level of the similarity.

With the optimization criterion of minimizing the beampattern ISL and the waveform energy over bands Ω_k ; $k = 1, \dots, K$, the problem of the transmit beampattern design under the PAR and similarity constraints can be formulated as

$$\begin{aligned} \min_{\mathbf{s}} \quad & \omega_c \frac{\mathbf{s}^H \mathbf{\Upsilon}_s \mathbf{s}}{\mathbf{s}^H \mathbf{\Upsilon}_m \mathbf{s}} + \sum_{k=1}^K \omega_k \mathbf{s}^H \mathbf{\Xi}^k \mathbf{s} \\ \text{s.t.} \quad & (\mathbf{s} - \mathbf{s}_0)^H (\mathbf{s} - \mathbf{s}_0) \leq \varepsilon^2 \\ & \mathbf{s}^H \mathbf{s} = 1 \\ & \mathbf{s}^H \mathbf{E}_n \mathbf{s} \leq \frac{\eta}{ML}, \quad n = 1, \dots, ML \end{aligned} \quad (12)$$

where ω_c is the weight for the beampattern ISL and ω_k is the weight for k th waveform energy in the k th band.

It can be seen that the above optimization problem, which involves a nonconvex objective function, a nonconvex quadratic equality constraint, and nonhomogeneous quadratic inequality constraints, is NP-hard [22]. Moreover, since the objective function in (12) includes both a quadratic fractional and quadratic functions, the Semi-Definite Relaxation (SDR) technique based on Charnes-Cooper transformation can not be thus exploited to solve it [13]. To this end, an iterative algorithm is developed to tackle the problem in (12).

3. SOLUTION TO THE OPTIMIZATION PROBLEM

In this section, we shall present an iterative algorithm, which is named A-ADMM, to tackle the problem in (12).

Before proceeding, we rewrite the problem in (12) in a

real-valued form as

$$\begin{aligned} \min_{\mathbf{s}_r} & \omega_c \frac{\mathbf{s}_r^T \mathbf{\Upsilon}_{sr} \mathbf{s}_r}{\mathbf{s}_r^T \mathbf{\Upsilon}_{mr} \mathbf{s}_r} + \sum_{k=1}^K \omega_k \mathbf{s}_r^T \mathbf{\Xi}_r^k \mathbf{s}_r \\ \text{s.t.} & (\mathbf{s}_r - \mathbf{s}_{0r})^T (\mathbf{s}_r - \mathbf{s}_{0r}) \leq \varepsilon^2, \\ & \mathbf{s}_r^T \mathbf{s}_r = 1, \\ & \mathbf{s}_r^T \mathbf{E}_n^r \mathbf{s}_r \leq \frac{\eta}{ML}, n = 1, \dots, ML. \end{aligned} \quad (13)$$

where \mathbf{s}_{0r} , \mathbf{s}_r , $\mathbf{\Upsilon}_{sr}$, $\mathbf{\Upsilon}_{mr}$, $\mathbf{\Xi}_r^k$ and \mathbf{E}_n^r are the real-valued forms of \mathbf{s}_0 , \mathbf{s} , $\mathbf{\Upsilon}_s$, $\mathbf{\Upsilon}_m$, $\mathbf{\Xi}^k$ and \mathbf{E}_n , respectively.

The key of the proposed algorithm is to modify the problem in (13) by introducing an auxiliary primal variable \mathbf{h}_r as

$$\begin{aligned} \min_{\mathbf{s}_r, \mathbf{h}_r} & \omega_c \frac{\mathbf{s}_r^T \mathbf{\Upsilon}_{sr} \mathbf{h}_r}{\mathbf{s}_r^T \mathbf{\Upsilon}_{mr} \mathbf{h}_r} + \sum_{k=1}^K \omega_k \mathbf{s}_r^T \mathbf{\Xi}_r^k \mathbf{h}_r \\ \text{s.t.} & \mathbf{s}_r - \mathbf{h}_r = \mathbf{0} \\ & \mathbf{s}_r^T \mathbf{h}_r = 1, \\ & (\mathbf{s}_r - \mathbf{s}_{0r})^T (\mathbf{h}_r - \mathbf{s}_{0r}) \leq \varepsilon^2, \\ & \mathbf{s}_r^T \mathbf{E}_n^r \mathbf{h}_r \leq \frac{\eta}{ML}, n = 1, \dots, ML. \end{aligned} \quad (14)$$

As a consequence, the non-convex objective function in (13) has been converted to a bi-quasiconvex function and bi-linear function with respect to each primal variable. Moreover, the non-convex quadratic equality constraint in (13) is modified as a bi-affine equality, i.e., jointly affine in \mathbf{s}_r and \mathbf{h}_r . In addition, the quadratic inequality constraints have been converted to linear inequality constraints. Therefore, the ADMM algorithm can be exploited to solve the problem in (14) [19].

Under the ADMM framework, instead of always maintaining equality constraints, the equality constraints are placed in the augmented Lagrangian function of the primitive function. More exactly, the augmented Lagrangian of (14) is written as

$$\begin{aligned} \mathcal{L}(\mathbf{s}_r, \mathbf{h}_r, \mathbf{u}, \mathbf{v}) &= F(\mathbf{s}_r, \mathbf{h}_r) + \mathbf{s}_r^T \mathbf{G} \mathbf{h}_r + \mathbf{u}^T (\mathbf{s}_r - \mathbf{h}_r) \\ &+ \frac{\rho_1}{2} \|\mathbf{s}_r - \mathbf{h}_r\|^2 + \mathbf{v} (\mathbf{s}_r^T \mathbf{h}_r - 1) + \frac{\rho_2}{2} \|\mathbf{s}_r^T \mathbf{h}_r - 1\|^2 \end{aligned} \quad (15)$$

where $F(\mathbf{s}_r, \mathbf{h}_r)$ and \mathbf{G} are, respectively, defined as

$$F(\mathbf{s}_r, \mathbf{h}_r) \triangleq \omega_c \frac{\mathbf{s}_r^T \mathbf{\Upsilon}_{sr} \mathbf{h}_r}{\mathbf{s}_r^T \mathbf{\Upsilon}_{mr} \mathbf{h}_r} \quad \text{and} \quad \mathbf{G} = \sum_{k=1}^K \omega_k \mathbf{\Xi}_r^k$$

and \mathbf{u} and \mathbf{v} are dual variables, $\rho_1, \rho_2 > 0$ are penalty parameters which place a penalty on the violations of primal feasibility. Hence, at the $(k+1)$ th iteration, the ADMM algorithm consists of the following update procedures [19]:

$$\mathbf{s}_r^{k+1} = \arg \min_{\mathbf{s}_r \in \mathcal{D}_s} \mathcal{L}(\mathbf{s}_r, \mathbf{h}_r^k, \mathbf{u}^k, \mathbf{v}^k) \quad (16)$$

$$\mathbf{h}_r^{k+1} = \arg \min_{\mathbf{h}_r \in \mathcal{D}_h} \mathcal{L}(\mathbf{s}_r^{k+1}, \mathbf{h}_r, \mathbf{u}^k, \mathbf{v}^k) \quad (17)$$

$$\mathbf{u}^{k+1} = \mathbf{u}^k + \rho_1 (\mathbf{s}_r^{k+1} - \mathbf{h}_r^{k+1}) \quad (18)$$

$$\mathbf{v}^{k+1} = \mathbf{v}^k + \rho_2 (\mathbf{s}_r^{k+1 T} \mathbf{h}_r^{k+1} - 1) \quad (19)$$

where \mathcal{D}_s and \mathcal{D}_h are two sets, respectively, defined as

$$\begin{aligned} \mathcal{D}_s &\triangleq \left\{ \mathbf{s}_r \mid \begin{array}{l} \mathbf{s}_r^T \mathbf{E}_n^r \mathbf{h}_r^k \leq \eta/ML, n = 1, 2, \dots, ML. \\ (\mathbf{s}_r - \mathbf{s}_{0r})^T (\mathbf{h}_r^k - \mathbf{s}_{0r}) \leq \varepsilon^2, \end{array} \right\} \\ \mathcal{D}_h &\triangleq \left\{ \mathbf{h}_r \mid \begin{array}{l} (\mathbf{s}_r^{k+1})^T \mathbf{E}_n^r \mathbf{h}_r \leq \eta/ML, n = 1, 2, \dots, ML. \\ (\mathbf{s}_r^{k+1} - \mathbf{s}_{0r})^T (\mathbf{h}_r - \mathbf{s}_{0r}) \leq \varepsilon^2 \end{array} \right\} \end{aligned}$$

In the sequel, the solutions to the alternating minimization problems from (16) and (17) are presented.

It is noted that the augmented Lagrangian function in (15) consists of two parts, i.e., $F(\mathbf{s}_r, \mathbf{h}_r)$ and the remaining quadratic function term. Unfortunately, $F(\mathbf{s}_r, \mathbf{h}_r^k)$ is a quasi-convex function with respect to \mathbf{s}_r [22], and it is challenging to directly solve the problems in (16) and (17). Nevertheless, the epi-graph of a quasi-convex function is convex [22], and hence, the primal variable \mathbf{s}_r can be achieved through minimizing the approximated function of $F(\mathbf{s}_r, \mathbf{h}_r^k)$ [18]. Consequently, the update formula for the primal variable \mathbf{s}_r in A-ADMM replaces the exact minimization in (16) by the minimization of the quadratic form

$$\begin{aligned} \mathbf{s}_r^{k+1} &= \arg \min_{\mathbf{s}_r \in \mathcal{D}_s} F(\mathbf{s}_r^k, \mathbf{h}_r^k) + \nabla_{\mathbf{s}_r}^T F(\mathbf{s}_r^k, \mathbf{h}_r^k) (\mathbf{s}_r - \mathbf{s}_r^k) \\ &+ \frac{\tau}{2} \|\mathbf{s}_r - \mathbf{s}_r^k\|^2 + \mathbf{s}_r^T \mathbf{G} \mathbf{h}_r^k + \mathbf{u}^T (\mathbf{s}_r - \mathbf{h}_r^k) \\ &+ \frac{\rho_1}{2} \|\mathbf{s}_r - \mathbf{h}_r^k\|^2 + \mathbf{v} (\mathbf{s}_r^T \mathbf{h}_r^k - 1) + \frac{\rho_2}{2} \|\mathbf{s}_r^T \mathbf{h}_r^k - 1\|^2 \end{aligned} \quad (20)$$

where τ is a given positive constant. It is noticed that the problem in (20) is a Quadratic Programming (QP) problem, whose closed-form solution can be obtained by solving the associated Karush-Kuhn-Tucker (KKT) conditions [22] or the Active-Set Method (ASM) [23].

Due to the symmetry of \mathbf{h}_r and \mathbf{s}_r , \mathbf{h}_r can be updated similarly to the update procedure of \mathbf{s}_r .

In each iteration, the update of \mathbf{s}_r^k needs computing $\nabla_{\mathbf{s}_r} F(\mathbf{s}_r, \mathbf{h}_r^k)$ and solving KKT conditions. Their computational complexity are $\mathcal{O}(M^2 L^2)$ and $\mathcal{O}(M^3 L^3)$ [24], respectively. In summary, in each iteration, the multiplications of the proposed algorithm is $\mathcal{O}(M^3 L^3)$.

4. NUMERICAL RESULTS

Now, numerical simulations are provided to assess the performance of the proposed algorithm. We assume that a colocated narrow band MIMO radar with a uniform linear array (ULA) comprising $M = 8$ transmit antennas, the inter-element spacing is half-wavelength. In particular, we consider the orthogonal frequency division multiplexing linear frequency modulation (OFDM-LFM) signal as the reference waveform, whose total bandwidth is $Bw = 2$ MHz with a sampling frequency of $f_s = 2$ MHz, the frequency interval $\Delta f = Bw/M$, and

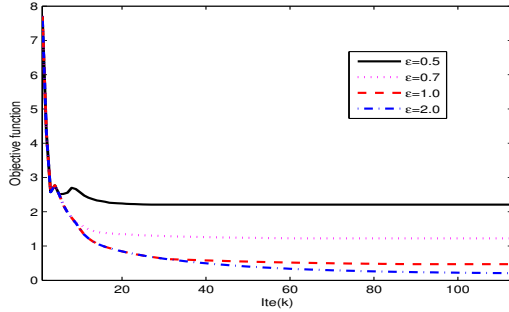


Fig. 1. The values of objective function versus the iteration number for $\eta = 1.1$ and $\varepsilon = 0.5, 0.7, 1.0, 2.0$.

the pulse width $T_p = 32 \mu s$, which results in $L = 64$ samples. The PAR value $\eta = 1.1$. We consider the following normalized baseband equivalent radar stopbands, which are $(0, 0.08)$, $(0.3, 0.39)$, $(0.63, 0.7)$, $(0.9, 1)$, and one mainlobe scenario with mainlobe region $[-10^\circ, 10^\circ]$ and sidelobe region $[-90^\circ, -10^\circ] \cup [10^\circ, 90^\circ]$ and a mesh grid size of 1° . Furthermore, we set $\mathbf{h}_r^0 = \mathbf{s}_r^0$, $\mathbf{u}^0 = \mathbf{0}$ and $\mathbf{v}^0 = 0$. The penalty parameters ρ_1, ρ_2 are set to $\rho_1 = \rho_2 = 10$ and τ in (20) is chosen to be 1. As to the weights in (12), we set $\omega_k = \omega_k = 1, k = 1, \dots, K$.

Fig. 1 depicts the values of objective function in (12) versus the iteration number for similarity level $\varepsilon = 0.5, 0.7, 1.0, 1.5$. It is seen from Fig. 1 that the values of the objective function can converge to the local best value, and the values decrease with the similarity values ε . This observation agrees with our expectations. Interestingly, Fig. 1 also shows that the ε will affect the convergence speed, and the larger the ε , the slower the algorithm converges.

Next, Fig. 2 displays the resulting beampatterns with different similarity values for one mainlobe case. The blue curve shows the beampattern of the OFDM-LFM, and it is well known that the beampattern of the OFDM-LFM is omnidirectional due to the orthogonality. As expected, Fig. 2 also shows that the higher the ε , the higher the degree of freedom of waveform at design stage. As a result, the lower the sidelobe level will be achieved.

In addition, the ESDs of the designed waveforms versus the normalized frequency are shown in Fig. 3, together with that of the OFDM-LFM. The stop-bands are shaded in light gray. As expected, the nulls of the ESD become deeper as the similarity degree is lowered, which again is due to the more degrees of freedom in the optimization problem.

Finally, the pulse compression property of each designed waveform is compared with that of the reference OFDM-LFM in Fig. 4. The computational procedure of pulse compression can be found in [13]. The results, as expected, display that the sidelobe level increases with ε . This is consistent with the results reported in [13].

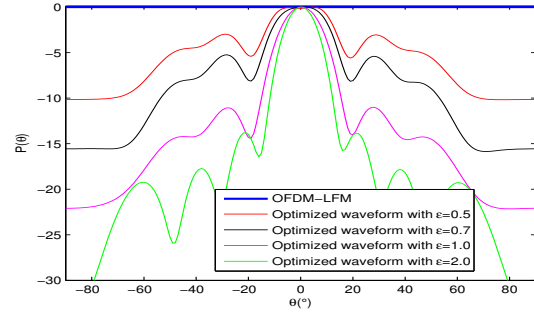


Fig. 2. The beampattern behaviors for one mainlobe case considering $\eta = 1.1$ and $\varepsilon = 0.5, 0.7, 1.0, 2.0$

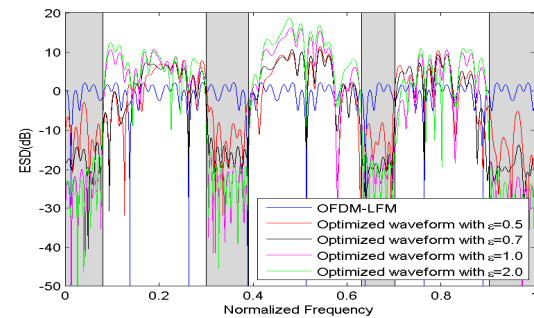


Fig. 3. ESDs (dB) versus normalized frequency for $\eta = 1.1$ and $\varepsilon = 0.5, 0.7, 1.0, 2.0$.

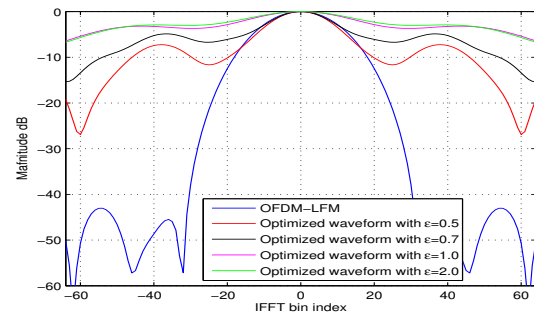


Fig. 4. The pulse compression properties of the waveforms compared with OFDM-LFM for $\eta = 1.1$ and $\varepsilon = 0.5, 0.7, 1.0, 2.0$.

5. CONCLUSION

In this paper, the problem of the spectrally compatible waveform design for MIMO radar transmit beampattern under the PAR and similarity constraints has been addressed. In order to tackle the resultant problem, the A-ADMM algorithm has been devised to solve the modified problem. Results have revealed that the proposed algorithm is able to realize a compromise between the spectral compatibility, the beampattern behavior and the pulse compression property.

6. REFERENCES

- [1] K. Forsythe and D. Bliss, "Waveform correlation and optimization issues for MIMO radar," in *Proc. 39th Asilomar Conf. Signals, Syst. Comput.*, Nov. 2005, pp. 1306–1310.
- [2] W. Roberts, H. He, J. Li, "Probing waveform synthesis and receiver filter design," *IEEE Signal Process. Mag.*, pp. 99–112, July. 2010.
- [3] P. Stoica, J. Li, and Y. Xie, "On probing signal design for MIMO radar," *IEEE Trans. Signal Process.*, vol. 55, no. 8, pp. 4151–4161, 2007.
- [4] P. Stoica, J. Li, and X. Zhu, "Waveform synthesis for diversity-based transmit beampattern design," *IEEE Trans. Signal Process.*, vol. 56, no. 6, pp. 2593–2598, 2008.
- [5] J. Li, P. Stoica, and X.-Y. Zheng, "Signal synthesis and receiver design for MIMO radar imaging," *IEEE Trans. Signal Process.*, vol. 56, no. 8, pp. 3959–3968, 2008.
- [6] J. Lipor, S. Ahmed, and M. M. Alouini, Fourier-based transmit beampattern design using MIMO radar, *IEEE Trans. Signal Process.*, vol. 62, no. 9, pp. 2226–2235, Apr. 2014.
- [7] T. Bouchoucha, S. Ahmed, and M. S. Alouini, DFT-based closedform covariance matrix and direct waveforms design for MIMO radar to achieve desired beampatterns, *IEEE Trans. Signal Process.*, vol. 62, no. 9, pp. 2104–2113, Jan. 2017.
- [8] X. Zhang, Z. He, L. Bacchus, and J. Yan, "MIMO radar transmit beampattern matching design," *IEEE Trans. Signal Process.*, vol. 63, no. 8, pp. 2049–2056, Apr. 2015.
- [9] Z. Cheng, Z. He, S. Zhang, and J. Li, "Constant modulus waveform design for MIMO radar transmit beampattern," *IEEE Trans. Signal Process.*, vol. 65, no. 18, pp. 4912–4923, 2017.
- [10] D. W. Bliss and K. W. Forsythe, "Multiple-input multiple-output (MIMO) radar and imaging: Degrees of freedom and resolution," in *Proc. 37th Asilomar Conf. Signals, Syst., Comput.*, Pacific Grove, CA, Nov. 2003, vol. 1, pp. 54–59.
- [11] N. H. Lehmann, A. M. Haimovich, R. S. Blum, and L. Cimini, "High resolution capabilities of MIMO radar," in *Proc. 38th Asilomar Conf. Signals, Syst., Comput.*, Pacific Grove, CA, Nov. 2006, pp. 25–30.
- [12] E. Fishler, A. Haimovich, and R. Blum, "Spatial diversity in radars models and detection performance," *IEEE Trans. Signal Process.*, vol. 54, no. 3, pp. 823–838, 2007.
- [13] G. Cui, H. Li, and M. Rangaswamy, "MIMO radar waveform design with constant modulus and similarity constraints," *IEEE Trans. Signal Process.*, vol. 62, no. 2, pp. 343–353, 2014.
- [14] G. Cui, X. Yu, and V. Carotenuto, and L. Kong, "Space-time transmit code and receive filter design for colocated MIMO radar," *IEEE Trans. Signal Process.*, vol. 65, no. 5, pp. 1116–1129, 2017.
- [15] A. Aubry, A. De Maio, M. Piezzo, and A. Farina, "Radar waveform design in a spectrally crowded environment via non-convex quadratic optimization," *IEEE Trans. Aerosp. Electron. Syst.*, vol. 50, no. 2, pp. 1138–1152, April 2014.
- [16] A. Aubry, A. De Maio, Y. Huang, M. Piezzo, and A. Farina, "A new radar waveform design algorithm with improved feasibility for spectral coexistence," *IEEE Trans. Aerosp. Electron. Syst.*, vol. 51, no. 2, pp. 1029–1038, April 2015.
- [17] A. Aubry, V. Carotenuto, and A. De Maio, "Forcing multiple spectral compatibility constraints in radar waveforms," *IEEE Signal Process. Lett.*, vol. 23, no. 4, pp. 483–487, April 2016.
- [18] M. Hong, M. Razaviyayn, Z. Q. Luo, and J.-S. Pang, "A unified algorithmic framework for block-structured optimization involving big data: With applications in machine learning and signal processing," *IEEE Signal Process. Mag.*, vol. 33, no. 1, pp. 57–77, 2016.
- [19] S. Boyd, N. Parikh, E. Chua, B. Peleato, and J. Eckstein, "Distributed optimization and statistical learning via the alternating direction method of multipliers," *Found. Trend. Mach. Learn.*, vol. 3, no. 1, pp. 1–122, 2011.
- [20] Z. Cheng, Z. He, B. Liao, and Min Fang, "MIMO Radar Waveform Design With PAPR and Similarity Constraints," *IEEE Trans. Signal Process.*, vol. 66, no. 4, pp. 968–981, 2018.
- [21] A. De Maio, S. De Nicola, Y. Huang, D. P. Palomar, S. Zhang, and A. Farina, "Code design for radar STAP via optimization theory," *IEEE Trans. Signal Process.*, vol. 58, no. 2, pp. 679–694, 2010.
- [22] S. Boyd and L. Vandenberghe, *Convex optimization*, Cambridge, U.K.: Cambridge Univ. Press, 2004.
- [23] J. Nocedal and S. J. Wright, *Numerical Optimization*. Springer, 1999.
- [24] M. Zhao, Y. Cai, Q. Shi, and B. Champagne, "Robust transceiver design for MISO interference channel with energy harvesting," *IEEE Trans. Signal Process.*, vol. 64, no. 17, pp. 4618–4633, 2016.